A Hands-On SAXS Tutorial for Particle-Based Soft Materials

Thomas Gibaud[1, *]

[1] *Univ Lyon, Ens de Lyon, CNRS, Laboratoire de Physique, 69342 Lyon, France*

(Dated: October 20, 2026)

Small-angle X-ray scattering (SAXS) provides a direct probe of structure over nanometre to sub-micrometre length scales and is widely used to characterize particle-based soft materials. This tutorial provides a hands-on introduction to the analysis and interpretation of SAXS data, with particular emphasis on connecting scattering features to particle structure, interparticle interactions, and collective organization. Using silica nanoparticle suspensions as a starting point, we introduce background subtraction, absolute intensity normalization, the scattering invariant, volume fraction determination, and form-factor analysis. We then consider salt-induced colloidal gelation and examine the evolution of the structure and rheological properties during gel formation using fractal and asymptotic models. Finally, we discuss SAXS from concentrated hard-sphere-like suspensions, focusing on the structure factor, compressibility, interparticle correlations, and the emergence of glassy behavior. Throughout, the emphasis is on practical data analysis and on developing a physical understanding of the information contained in SAXS measurements.

Please bring your laptop equipped with at least one software for basic data manipulation, and pre-install SasView from `https://sasview.org`. Having access to MATLAB, Python, or alternative data analysis softwares is highly recommended for more advanced analysis. Please download the tutorial data at `https://perso.ens-lyon.fr/thomas.gibaud/cocogelsaxs/`

I. INTRODUCTION

Small-angle X-ray scattering (SAXS) is a powerful technique for probing the structure of soft materials over length scales ranging from a few nanometres to hundreds of nanometres. Because the scattered intensity contains information about both the individual particles and their spatial organization, SAXS can be used to investigate particle size and shape, interparticle correlations, aggregation, gelation, and phase transitions.

The interpretation of SAXS data, however, requires more than fitting a scattering curve with a model. Experimental normalization and background subtraction must first be carefully considered, while the separation of particle form factors from collective structure requires measurements over an appropriate range of concentrations and wavevectors. Moreover, apparently simple features of a scattering curve, such as a low-q upturn or a peak in the structure factor, can originate from very different physical mechanisms. Establishing the connection between these features and the underlying structure is therefore an essential part of SAXS analysis.

This tutorial develops this approach through a series of practical examples. We first analyze dilute silica nanoparticle suspensions to introduce basic SAXS concepts, including background subtraction, the scattering invariant, volume fraction, and particle form factors. We then consider the destabilization and gelation of silica nanoparticles following the addition of salt, using the evolution of the scattering intensity and rheological response to connect microscopic aggregation with the formation of a space-spanning network. Fractal and asymptotic descriptions are introduced to characterize the structures that emerge during gelation. Finally, we examine concentrated hard-sphere-like suspensions and use the structure factor to discuss interparticle correlations and compressibility.

The objective is not to provide an exhaustive review of SAXS analysis, but rather to develop a practical framework in which scattering data, mathematical models, and physical interpretation are considered together. The exercises are designed to encourage the reader to move from raw experimental data to quantitative structural information and, ultimately, to a physical description of the material.

II. FROM RAW DATA TO FORM FACTOR

Small-angle X-ray scattering is used to characterize aqueous silica nanoparticle (Ludox SM) suspensions. Four samples of weight concentrations c_w are measured in quartz capillary of with width $e = 2$ mm (see Tab. I and Fig. 1).

* thomas.gibaud@ens-lyon.fr

Sample	c_w ($wt\%$)	Data file
LudoxHS	0.0025	`I_HS1.txt`
LudoxHS	0.025	`I_HS2.txt`
LudoxHS	0.25	`I_HS3.txt`
LudoxHS	1	`I_HS4.txt`
Water	/	`I_water.txt`

Table I. SAXS datasets.

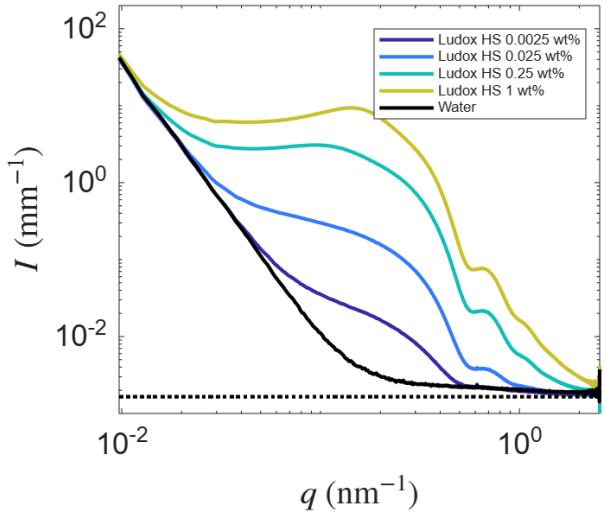


Figure 1. SAXS intensity $I(q)$ normalized by the capillary width for Ludox HS suspensions at different silica concentrations and for water.

A. Raw data

1. Load the five experimental datasets and plot the measured intensities $I(q)$ in mm^{-1} on a log–log scale after dividing the raw intensity by the capillary width e.
2. Why is this normalization by e necessary?
3. At large q, do the silica samples approach the water scattering curve? Discuss the physical origin of this behavior. What is the expected water scattering intensity at $q \simeq 1$ nm^{-1} [1]?

B. Background subtraction

The scattering intensity from the silica suspension is approximated by

$$I(q) = \frac{I_{\text{sample}}(q)}{e} - \alpha \frac{I_{\text{water}}(q)}{e}.$$

1. Ideally, what should be the value of α?
2. Plot the resulting $I(q)$ on a log–log scale. Why is a logarithmic representation useful for SAXS data?
3. How can you assess whether the background subtraction is correct? Plot $q^2 I(q)$ and $q^4 I(q)$. How are those representation useful?

C. Absolute intensity, invariant and volume fraction

1. Show that the volume fraction corresponding to the mass fraction c_w is

$$\phi_{c_w} = \frac{c_w/d_{\text{SiO}_2}}{c_w/d_{\text{SiO}_2} + (1-c_w)/d_w},$$

with densities $d_{\text{SiO}_2} = 2.2$ g cm^{-3} and $d_w = 1.0$ g cm^{-3}.

2. For a two-phase system, the scattering invariant [2–5] is

$$Q = \int_0^\infty q^2 I(q)\, dq = 2\pi^2 r_e^2 (\Delta\rho_e)^2 \phi(1-\phi),$$

where $r_e = 2.871 \times 10^{-6}$ nm is the classical electron radius and $\Delta\rho_e = \rho^e_{\text{SiO}_2} - \rho^e_w \simeq 318$ e nm^{-3}. Justify this value of $\Delta\rho_e$.

3. Calculate Q for each sample, taking care with the units, and determine the corresponding volume fraction from

$$\phi = \frac{1-\sqrt{1-4A}}{2} \text{ with } A = \frac{Q}{2\pi^2 r_e^2 (\Delta\rho_e)^2}.$$

Note: After background subtraction, $I(q)$ may occasionally become slightly negative, particularly at large or low q where the sample and background intensities are comparable. Such values are not physically meaningful and can significantly affect the numerical evaluation of the invariant Q. Care should therefore be taken when selecting the q-range used for the integration and when assessing the uncertainty associated with the background subtraction.

4. Plot ϕ_{c_w} versus ϕ obtained from the invariant. Discuss possible deviations arising from imperfect background subtraction, finite q-range, uncertainties in density or electron-density contrast, sample preparation, and instrumental normalization.
5. Plot $I(q)/\phi$ for all four concentrations on the same graph. Why do the curves collapse onto a master curve at large q, but not necessarily at small q?

D. Form factor

1. Which $I(q)$ dataset is best suited to determine the form factor of the nanosilica spheres?

2. Why is it useful to perform a dilution series when determining the form factor?

3. Fit the data using SasView. What parameters do you obtain, and how do they compare with the expected nanosilica size?

III. COLLOIDAL HARD-SPHERE

This tutorial aims to understand how the microscopic interaction between particles determines their structure, and how this structure can be probed using small-angle scattering. The system considered here is a concentrated suspension of charge-stabilized polystyrene (PS) spheres in glycerol (see Tab. II and Fig. 2 [6]) which behave as hard sphere colloidal system [7–9].

Sample	ϕ (%)	Data file
PS	0.027	`I_PS1.txt`
PS	0.13	`I_PS2.txt`
PS	0.28	`I_PS3.txt`
PS	0.34	`I_PS4.txt`
PS	0.49	`I_PS5.txt`
PS	0.52	`I_PS6.txt`

Table II. SAXS datasets.

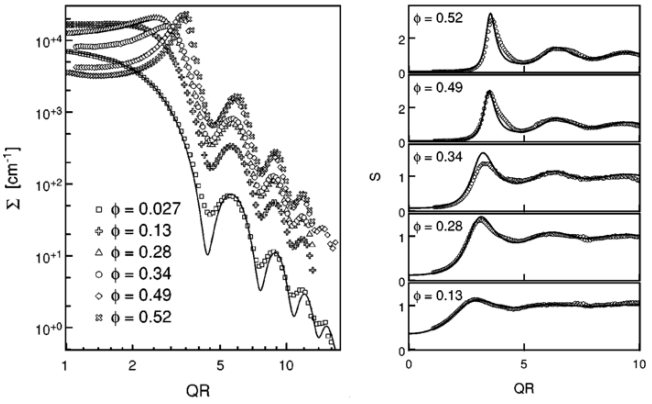


Figure 2. SAXS intensity $I(q)$ for charge-stabilized polystyrene (PS) spheres in glycerol at different volume fractions and their structure factor. Background solvent is already subtracted from the data.

A. What is a hard-sphere system?

1. Define a hard sphere in terms of its interparticle interaction and sketch the interaction potential $U(r)$ as a function of the center-to-center distance r between two particles.

2. What is the relevant physical parameters of a hard-sphere suspension that controls its phase diagram? Does the phase diagram of hard sphere depend on the temperature?

3. Explain it in term of free energy. More precisely, What is the free volume available to a particle? How does it change with increasing volume fraction ϕ?

4. How can the competition between the entropy of the disordered fluid and the free volume available in the ordered crystal drive the fluid–crystal transition?

B. What can we learn from the scattering intensity?

The measured scattering intensity is written schematically as $I(q) \propto P(q)S(q)$, where $P(q)$ is the particle form factor and $S(q)$ is the structure factor.

1. What information about the particles is contained in $P(q)$?

2. What information about the spatial organization of the particles is contained in $S(q)$?

3. Is the system monodisperse or polydisperse? What features of the scattering curves support your answer?

4. What features of $S(q)$ can provide information about the nature of the interparticle interactions?

C. What is the physical meaning of $S(0)$?

1. What does the limit $q \to 0$ correspond to in real space?

2. What does a large value of $S(0)$ compared to the value 1 indicate? What does a small value of $S(0)$ compared to the value 1 indicate?

3. Can $S(0)$ ever be exactly zero? What would this imply about density fluctuations?

4. For an equilibrium fluid, the static structure factor satisfies the compressibility equation. Why is $S(0)$ therefore related to the equation of state, $P(\phi)$ (for an ideal gas, $P \propto \phi$)?

5. Why does an interacting hard-sphere system deviate from the ideal-gas equation of state? Explain physically why the pressure increases more rapidly than the ideal-gas pressure as the volume fraction of hard spheres increases.

D. What it the meanning of the first correlation peak in $S(q)$?

1. A pronounced peak is observed in the structure factor especially at high ϕ. What is the physical origin of the peak in $S(q)$?
2. What does the position q^* of the peak tell you about the spatial organization of the particles?
3. Associate a characteristic real-space length with q^*: $\ell^* \simeq \frac{2\pi}{q^*}$. Is ℓ^* necessarily equal to the nearest-neighbor distance? Explain why or why not.
4. What information is contained in the height of the peak? What information is contained in its width?
5. How does the peak evolve when ϕ is increased? Justify $q^* \propto \phi^{1/3}$ [10].

E. Fit

One of the primary objectives of this section is to extract the effective hard-core particle size (d_0) and the thermodynamic packing fraction (ϕ) from dense colloidal suspensions via Small-Angle X-ray Scattering (SAXS) analysis. To achieve this, the structural arrangement of the interacting spheres must be accurately modeled through the structure factor, $S(q)$, which is fundamentally rooted in liquid-state theory. The spatial correlations of the fluid are governed by the Ornstein-Zernike (OZ) integral equation. To solve this mathematically underdetermined system, the Percus-Yevick (PY) closure relation, originally derived by Percus and Yevick [11], is applied. For ideal monodisperse hard spheres, this was solved analytically by Wertheim [12] and Thiele [13], and later expanded to multicomponent hard-sphere systems by Lebowitz [14]. When accounting for sizing parameters in realistic experimental distributions, structural calculations can be computed utilizing either the loose Gazzillo Scaling Approximation [15] or evaluated rigorously via Vrij's exact multicomponent solution [16], which can be coded efficiently using modern matrix reformulations [17].

1. What are the fundamental physical hypotheses behind the Percus-Yevick framework?
2. Fit the experimental scattering intensity, $I(q)$, within the OZ and PY framework. Explain why there are two radius in the fitting, the hard core particle radius and the effective particle radius. Beware that they are many variations of OZ-PY codes; make sure you understand the code you use.
3. How does $S(0)$ compare to the equation of state proposed by Carnahan-Starling for hard spheres [18], $\frac{P}{\rho k_B T} = \frac{1+\phi+\phi^2-\phi^3}{(1-\phi)^3}$, leading to $S(0) = \frac{(1-\phi)^4}{1+4\phi+4\phi^2-4\phi^3+\phi^4}$?
4. If the colloidal system has even mild size polydispersity ($s > 0.10$), the structural peak in $S(q)$ broadens and dampens. Discuss the physical difference between handling this using Vrij's exact multicomponent solution [16] versus using a local monodisperse approximation with a decoupling correction factor (like SasView's $\beta(q)$ method). Which framework preserves the true size-dependent cross-correlations and why?

IV. COLLOIDAL FRACTAL GELS

Rheo-SAXS is used to characterize the time evolution of an aqueous dispersion of Ludox SM nanoparticles in presence of NaCl as it forms a gel (see Tab. III [19] and Fig. 3).

Sample	t (s)	Data file
Ludoxgel	231	`I_gelserie1.txt`
Ludoxgel	731	`I_gelserie2.txt`
Ludoxgel	1231	`I_gelserie3.txt`
Ludoxgel	1731	`I_gelserie4.txt`
Ludoxgel	2231	`I_gelserie5.txt`
Ludoxgel	4731	`I_gelserie6.txt`

Table III. SAXS datasets.

A. Gelation of Ludox particles with addition of salt

1. Using the same silica particles as in the previous section, we now add salt. From an interaction point of view, explain why adding salt can destabilize the suspension and lead to gelation.
2. Why are equilibrium liquid-state theories, such as the Percus-Yevick approximation used for the Hard sphere in previous section, fundamentally inadequate for describing the structural properties of out-of-equilibrium colloidal gels [20, 21].
3. The data series Ludoxgel correspond to the scattering from a suspension of Ludox HS silica nanoparticles dispersed in water with NaCl at 500 mM, at $c_w = 10$ %w measured at as function of time t. The data files correspond to the viscous and elastic moduli, G'' and G', of the same dispersion as a function of time. Plot G' and G'' as a function of time. Plot $I(q,t)$ and $q^2 I(q,t)$ as a function of q. Plot $S(q)$ as a function of q.

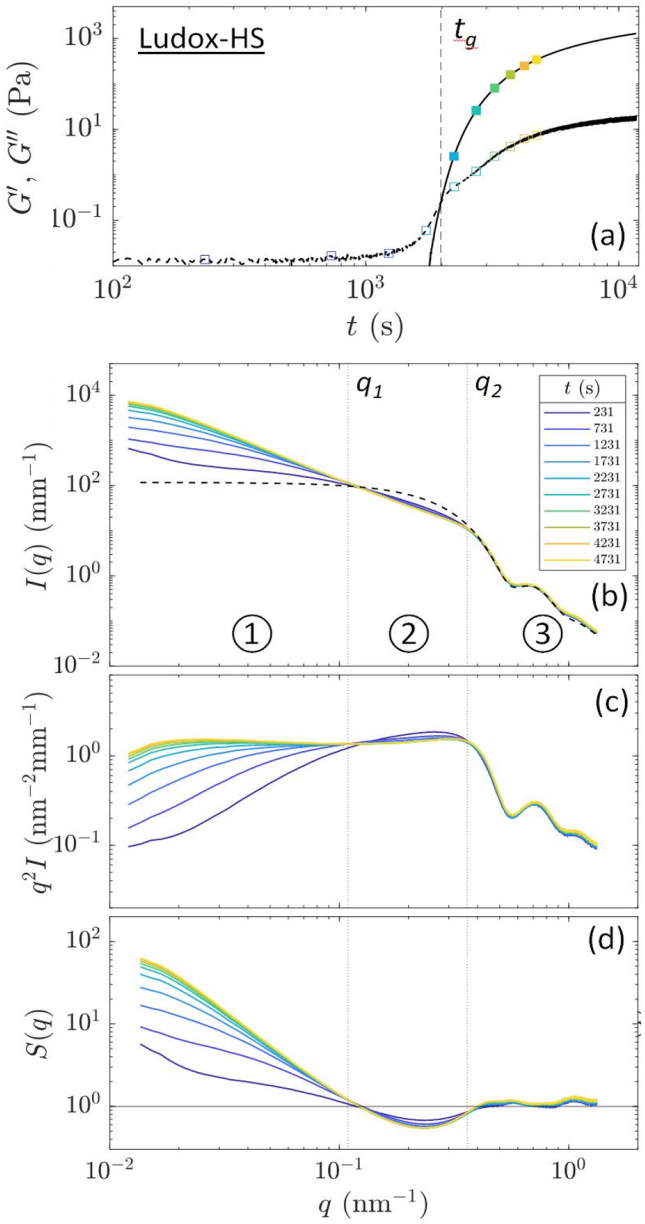


Figure 3. SAXS intensity $I(q)$ for gel as a function of time. Background solvent is already subtracted from the data.

4. Explain the emergence of strong forward scattering with time. Based on scaling arguments, what is the low-q structure that develops during gelation. For t=x determine its properties. Why does $S(q)$ exhibit a minimum below the baseline $S(q) = 1$? What does this minimum correspond to, and why does its intensity decrease with time? Make a sketch that illustrates the gelation process.

B. Fit of the data

1. Using a mass-fractal model [22–24], fit the data. The mass fractal model decomposes as follows, $I(q) = I_0, P(q), S(q)$ where $P(q)$ is the form factor of spherical silica nanoparticles, and $S(q) = 1 + \frac{d_f\,\Gamma(d_f-1)}{(q\xi)^{d_f}}\left[1+\frac{1}{(q\xi)^2}\right]^{\frac{1-d_f}{2}} \sin[(d_f-1)\arctan(q\xi)]$ is the mass-fractal structure factor. Here, d_f is the mass-fractal dimension, and ξ is the characteristic cluster size, related to the radius of gyration R_g by $R_g = \xi\sqrt{\frac{d_f(d_f+1)}{2}}$. Explain why the model can accurately describe either the low-q or the high-q regime, but not both simultaneously.

2. Develop an asymptotic model to describe the low-q data. Justify whether a Guinier–Porod approximation [25, 26] based on Beaucage's global unified framework [27], $I(q) = \begin{cases} I_0 \exp\left(-q^2 R_g^2/3\right), & q \le q_1, \\ I_P q^{-d_f}, & q > q_1, \end{cases}$ or an Ornstein–Zernike-type form generalized to a fractal exponent [28], $I(q) = \frac{I_0}{\left[1+(q\xi)^2\right]^{d_f/2}}$, is appropriate for describing the data. Fit the data and plot the fitting parameters as a function of time.

C. Other gels

1. The data in `I_supra.txt` corresponds to the scattering intensity from a viologen-based supramolecular gel exhibiting hierarchical self-assembly. From the high-q data, we get the smallest self-assembled structural unit in the hierarchy. Determine the shape and estimate the geometrical characteristics of this unit.

2. Propose a structure of the gel based on scaling argument and make a sketch that illustrate this structure.

[1] C. A. Dreiss, K. S. Jack, and A. P. Parker, On the absolute calibration of bench-top small-angle x-ray scattering instruments: a comparison of different standard methods, Applied Crystallography **39**, 32 (2006).

[2] G. Porod, Die Röntgenkleinwinkelstreuung von kolloiden Systemen. I. Teil, Kolloid-Zeitschrift **124**, 83 (1951).

[3] G. Porod, Die Röntgenkleinwinkelstreuung von kolloiden Systemen. II. Teil, Kolloid-Zeitschrift **125**, 51 (1952).

[4] L. A. Feigin and D. I. Svergun, *Structure Analysis by Small-Angle X-Ray and Neutron Scattering* (Plenum Press, 1987).

[5] O. Glatter and O. Kratky, eds., *Small Angle X-ray Scattering* (Academic Press, London, 1982).

[6] L. B. Lurio, D. Lumma, A. R. Sandy, M. A. Borthwick, S. G. J. Mochrie, A. Malik, M. Kennedy, and M. Sutton, Absence of de Gennes Narrowing in the Brownian Dynamics of Concentrated Colloidal Suspensions, Physical Review Letters **84**, 785 (2000).

[7] P. N. Pusey and W. van Megen, Phase behaviour of concentrated suspensions of nearly hard colloidal spheres, Nature **320**, 340 (1986).

[8] W. B. Russel, D. A. Saville, and W. R. Schowalter, *Colloidal Dispersions* (Cambridge University Press, Cambridge, 1989).

[9] G. Nägele, On the dynamics and structure of charge-stabilized colloidal suspensions, Physics Reports **272**, 215 (1996).

[10] F. Cousin, Small angle neutron scattering, in *EPJ web of conferences*, Vol. 104 (EDP Sciences, 2015) p. 01004.

[11] J. K. Percus and G. J. Yevick, Analysis of Kinetic Models for Electron Plasma Oscillations, Physical Review **110**, 1 (1958).

[12] M. S. Wertheim, Exact Solution of the Percus-Yevick Integral Equation for Hard Spheres, Physical Review Letters **10**, 321 (1963).

[13] E. Thiele, Equation of State for Hard Spheres, The Journal of Chemical Physics **39**, 474 (1963).

[14] J. L. Lebowitz, Exact Solution of Generalized Percus-Yevick Equation for a Mixture of Hard Spheres, Physical Review **133**, A895 (1964).

[15] D. Gazzillo, A. Giacometti, G. Della Valle, E. Venuti, and F. Carsughi, A scaling approximation for structure factors in the integral equation theory of polydisperse nonionic colloidal fluids, The Journal of Chemical Physics **111**, 7636 (1999).

[16] A. Vrij, Mixtures of hard spheres in the Percus–Yevick approximation. Light scattering at finite angles, The Journal of Chemical Physics **71**, 3267 (1979).

[17] R. Botet, R. Kwok, and B. Cabane, Percus–Yevick structure factors made simple, Journal of Applied Crystallography **53**, 1092 (2020).

[18] E. F. Carnahan and N. F. Starling, Equation of State for Noninteracting Hard Spheres, The Journal of Chemical Physics **51**, 635 (1969).

[19] A. Gibaud, W. J. Smit, S. Jamali, and T. Gibaud, Isosbestic points in time resolved saxs: from spectroscopic analogy to model free structural markers during colloidal gelation, arXiv preprint arXiv:2607.18954 (2026).

[20] M. Y. Lin, H. M. Lindsay, D. A. Weitz, R. C. Ball, R. Klein, and P. Meakin, Universality in colloid aggregation, Nature **339**, 360 (1989).

[21] C. M. Sorensen, Light scattering by fractal aggregates: a review, Aerosol Science and Technology **35**, 648 (2001).

[22] J. Teixeira, Small-angle scattering by fractal aggregates, Journal of Applied Crystallography **21**, 781 (1988).

[23] J. E. Martin and A. J. Hurd, Scattering from fractals, Journal of Applied Crystallography **20**, 61 (1987).

[24] T. Freltoft, J. Kjems, and S. Sinha, Power-law correlations and finite-size effects in silica particle aggregates studied by small-angle neutron scattering, Physical Review B **33**, 269 (1986).

[25] B. Hammouda, Analysis of the Beaucage model, Journal of Applied Crystallography **43**, 1474 (2010).

[26] B. Hammouda, A new Guinier–Porod model, Journal of Applied Crystallography **43**, 716 (2010).

[27] G. Beaucage, Approximations leading to a unified exponential/power-law approach to small-angle scattering, Journal of Applied Crystallography **28**, 717 (1995).

[28] M. E. Fisher and R. J. Burford, Theory of Critical Scattering. I. Direct Space Fluctuations and the Ornstein–Zernike Approximation, Physical Review **156**, 583 (1967).